https://doi.org/10.3311/PPci.19662

Periodica Polytechnica Civil Engineering, 66(3), pp. 785–797, 2022

Damage Characteristics of Argillaceous Quartz Sandstone Mesostructure under Different Wetting-drying Conditions

Lixu Deng[1,2,3], Jianfei Yang[1,2,3*], Guodong Zhang[1,2,3*], Yaxin Zhang[1,2,3], Guangfu Chen[1,2,3], Xijun Li[1,2,3]

[1] National Field Observation and Research Station of Landslides in Three Gorges Reservoir Area of Yangtze River, 443002, Yichang, Hubei, China
[2] College of Civil Engineering & Architecture, China Three Gorges University, 443002, Yichang, Hubei, China
[3] Hubei Geological Disaster Prevention and Control Engineering Technology Research Center, 443002, Yichang, Hubei, China
[*] Corresponding author, e-mail: yjf@ctgu.edu.cn; zgd@ctgu.edu.cn

Received: 07 December 2021, Accepted: 12 April 2022, Published online: 06 May 2022

Abstract

Extensive water–rock interaction in the Three Gorges Reservoir area of the Yangtze River leads to rock mass deterioration along the reservoir banks. However, mineral evolution behavior and its effect on the mesostructure deterioration of rocks under the wetting–drying cycle condition remain unknown. So, the wetting–drying cycle tests were conducted on peculiar argillaceous quartz sandstone in TGRA under neutral (pH = 7) and alkaline (pH = 10) water environments. Here, we provided detailed physical and microscopy images data to determine the control mechanism of mineral behavior on the evolution of sandstone's mesostructure. Under the neutral condition, repeated "absorption and swelling–dehydration and contraction" of clay minerals leads to the repeated physical action of "squeezing–unloading" in the interior of a rock. This results in the initiation and gradual expansion of cracks in the framework mineral quartz, exhibiting failure mode from the interior to the exterior. In contrast, under the alkaline condition, the dissolution on the surface of quartz particles leads to the expansion and connection of pores, implying that the sandstone exhibits failure mode from the exterior to the interior. Moreover, the internal mechanical analysis indicates the minerals are at high pressure because of the expansion of clay minerals in the neutral solution. However, in an alkaline water environment, the extrusion pressure of framework mineral quartz decreases significantly and is not easily broken due to increased porosity. Thus, the evolution behavior of minerals in different water environments plays an important role in the damage of the rock.

Keywords

mineral behavior, mesostructure, wetting–drying cycles, argillaceous quartz sandstone, rock deterioration

1 Introduction

Since the high water-level impoundment of the Three Gorges Reservoir area (TGRA) in 2008, the reservoir's water level has risen and fallen periodically between 145 m and 175 m above sea level every year, forming a 30 m hydro-fluctuation belt on the bank slope [1]. The rock and soil in the hydro-fluctuating zone have been affected by wetting–drying cycles because of the water level fluctuations [2]. Especially, the water–rock interaction under this special condition inevitably leads to the deterioration of rock mass in the hydro-fluctuation belt and then induces geological disasters on the reservoir bank slopes [3]. Therefore, studying the deterioration characteristics and laws of bank rocks under wetting–drying cycle conditions is not only one of the core components of the stability of reservoir bank slopes but also has important implications for the prevention, reduction, and treatment of reservoir bank slope disasters.

The bank slopes of TGRA are mostly distributed with sedimentary rocks (limestone, dolomite, marl, sandstone, siltstone, and mudstone), and a few magmatic rocks (granite) and metamorphic rocks (gneiss) [1]. Among these rocks, sandstone is one of the most widely distributed in the hydro-fluctuation belt. Previous studies have shown that the wetting–drying cycles exert a significant effect on sandstone deterioration, reflecting in the mechanical and physical properties, e.g., peak stress, internal friction angle, cohesion, porosity, acoustic emission, and wave speeds [4–9]. In addition, many studies concluded

Cite this article as: Deng, L., Yang, J., Zhang, G., Zhang, Y., Chen, Y., Li, X. "Damage Characteristics of Argillaceous Quartz Sandstone Mesostructure under Different Wetting-drying Conditions", Periodica Polytechnica Civil Engineering, 66(3), pp. 785–797, 2022. https://doi.org/10.3311/PPci.19662

that mineral composition, mesostructure, and rock structure are the primary reasons for the deterioration of sandstone under the wetting–drying cycles [10–12]. Intriguingly, under a distilled water environment and the same wetting–drying conditions (six cycles), the deterioration of siltstone is the most serious (uniaxial compressive strength decreases by approximately 81.0%) [13], that of shaly sandstone is the second (uniaxial compressive strength decreases by approximately 56.5%) [7], and that of feldspathic quartz sandstone is the least (uniaxial compressive strength decreases by approximately 14.0%) [14]. Thus, the mineral composition of sandstone is one of the decisive factors that influence its deterioration effect under wetting–drying cycles.

Due to the macroscopic mechanical properties of rocks being widely recognized to be determined by internal pore structures [15], the composition and behavior of minerals in the solution conditions are important factors that determine pore structures and control deterioration of the rock. So, different mesoscopic methods, such as Nuclear Magnetic Resonance (NMR), scanning electron microscope (SEM) imaging and digital image correlation (DIC) techniques [9–10, 12, 16], have been used to explore the mechanism of rock (granite, argillaceous rocks, sandstone, and so on) degradation. Although the relationship between the mesostructure changes and the mechanical properties have been investigated [5–6, 10], the relationship between the mesostructure and of mineral behaviors under the wetting–drying cycles are still unclear. On the flipside, a special sandstone, argillaceous quartz sandstone (which contains only quartz and clay minerals), is found on the reservoir bank slope near the Kamenziwan landslide in the TGRA. The argillaceous quartz sandstone has a relatively simple mineral composition compared with other types of sandstone with complex mineral compositions [5, 7]. It cannot only be used as an excellent experiment object for determining the evolution behavior of minerals under wetting–drying cycle conditions, but it can also provide a rare research opportunity for further exploring how minerals control the internal pore structure evolution process of sandstone. Therefore, our study aims to discover the evolution behavior of minerals in argillaceous quartz sandstone under different wetting–drying cycle conditions. On this basis, the control mechanism of mineral behaviors on the evolution of the mesostructure of sandstone is further introduced to discuss the deterioration characteristics and laws of sandstone under different water environments.

2 Materials and methods

2.1 Specimen preparation

The argillaceous quartz sandstone specimens used in this study were collected from the fluctuation zone of a typical bank slope in TGRA, China (Fig. 1(a)). To reduce errors during the experiments, all the specimens were obtained from one complete core (depth: 13–14 m) from a horizontal borehole (elevation: 171.2 m) located at the confluence of the Yangtze River and the Xietan River (Figs. 1(b) and 1(c)). The specimens were processed into cylinders with a diameter of 50 ± 0.2 mm and a height of 25 ± 0.2 mm (Fig. 1(d)). The surface flatness of the specimens met the standard in accordance with the International Society for Rock Mechanics (ISRM) [17].

Some essential physical properties of this sandstone were measured: dry density (2.53 g/cm^3), water absorption (0.80%), and porosity (3.74%). And the mesostructures of the specimens are shown in Figs. 2(a) and 2(b). The mineralogical composition of this sandstone determined via X-ray diffraction analysis indicates that this sandstone is primarily composed of quartz (69.8%), kaolinite (16.3%), illite (12.4%), and montmorillonite (1.5%) (Fig. 2(c)).

2.2 Experiment instrument

The pore structures of the sandstone specimens were measured using the NMR instrument (MacroMR12-150H-I, Niuman Corporation, China). The working environment and parameters of the NMR instrument were determined strictly in accordance with the operating specifications [10].

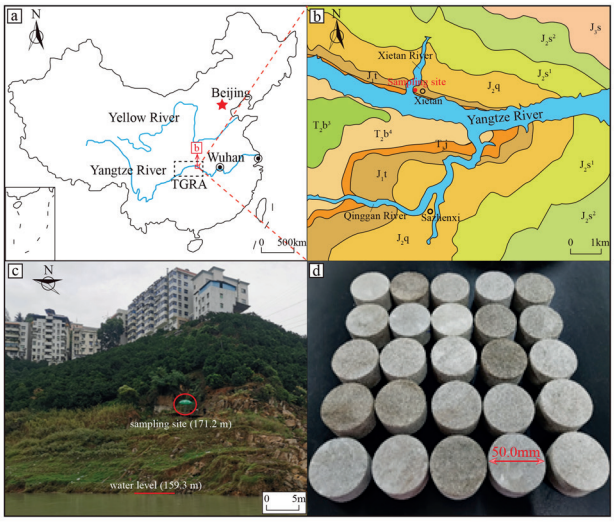

Fig. 1 Specimen sampling; (a) location of TGRA, (b) strata distribution in the sampling area, (c) bank slope of sampling site, (d) standard specimens

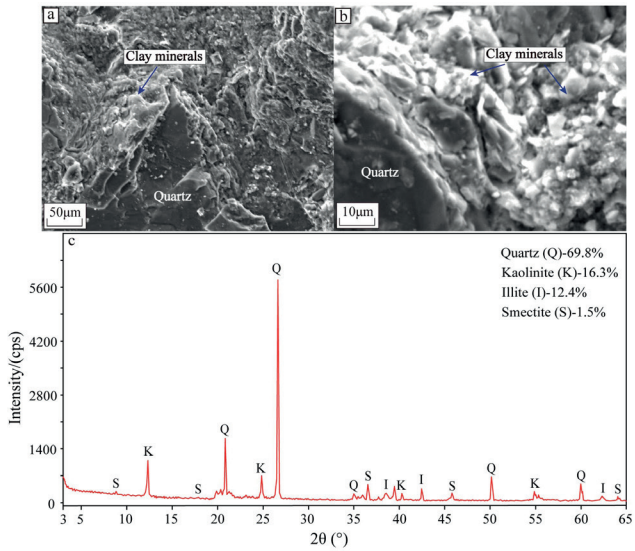

Fig. 2 Mesostructure and mineral test results

The NMR instrument magnetizes H atoms in water by applying a magnetic field, causing the H nucleus to resonate and absorb energy. When the external magnetic field disappears, the magnetized H nucleus releases energy. In this process, the time of releasing energy (i.e., relaxation time) is significantly different due to the varying H atom contents, which can be recorded as T_2 spectra via mathematical fitting [18]. Therefore, the porosity, pore size, and pore number of saturated rocks can be determined accurately and quantificationally via NMR; that is, the longer the relaxation time, the larger the pore size, the higher the signal amplitude, and the more pores [19].

The mesostructure and mineral morphology of the sandstone specimens were scanned via field emission scanning electron microscopy (SEM) by using JSM-IT300HR microscope (Sample Solution Corporation, China). The surface of the specimens was dusted and sprayed with gold before the tests.

2.3 Experiment methodology

Self-designed double-bucket circulation equipment was used in the wetting–drying cycle tests (Fig. 3) to better simulate the existing environment of reservoir bank rock mass (e.g., high water–rock ratio, dynamic state of water). In this equipment, the large bucket (50 L) was the liquid storage bucket used to simulate the water environment of the reservoir area. The small bucket (5 L) was the reaction bucket used to simulate the water–rock interaction environment within a small range of reservoir slope. In addition, two sealed barrels were connected by four corrosion-resistant BPT rubber hoses and two peristaltic

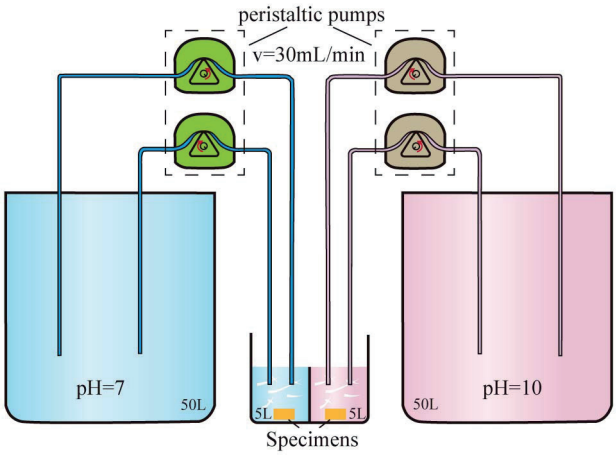

Fig. 3 Schematic diagram of double-bucket circulation test system

pumps. During the soaking process, the peristaltic pumps were adjusted to ensure that the solution would circulate in the two barrels at the same flow velocity (50 mL/min).

Due to long-term geological weathering and blooms of phytoplankton caused by eutrophication of water bodies [20–21], the Yangtze Rivers in nature is generally weakly alkaline (approximately 7.80–8.36) [22]. Meanwhile, the variation range of water pH values in most regions of TGRA is small (approximately 0.3) [22]. Therefore, the fluctuation range of pH value of the solution was strictly controlled within 0.3 in this experiment. In addition, considering that the reservoir water was alkalescent, and to control the experiment period, the pH value of the alkaline solution in this experiment was determined to be 10. Finally, the rock mass from the hydro-fluctuation belt in TGRA was exposed from May to October and soaked from October to May [1]. Therefore, the time ratio between the soaking and drying of the specimens in a wetting–drying cycle was 7:5 in this experiment.

The experimental procedures were as follows. (1) The sandstone specimens were dried in a 25 ℃ oven until the weight became constant. (2) The specimens that exhibited high similarity in terms of morphology, P-wave velocity, and T_2 spectrum were selected (Fig. 4). Then, the chosen specimens were divided into three groups: the original group (three specimens), the neutral environment group (six specimens), and the alkaline environment group (six specimens). (3) Two sets of double-bucket circulation equipment were filled with two kinds of solution: pH = 10 (NaOH) and pH = 7 (deionized water). Then, the specimens in the alkaline environment group (pH = 10) and the neutral environment group (pH = 7) were soaked and the peristaltic pumps were opened. (4) After soaking for 35 h (rock specimens can reach saturation in approximately 14 h), the specimens

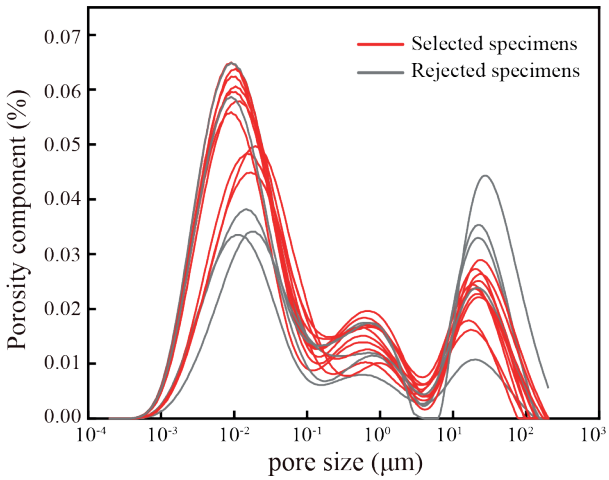

Fig. 4 T_2 spectrum distributions of original rock specimens

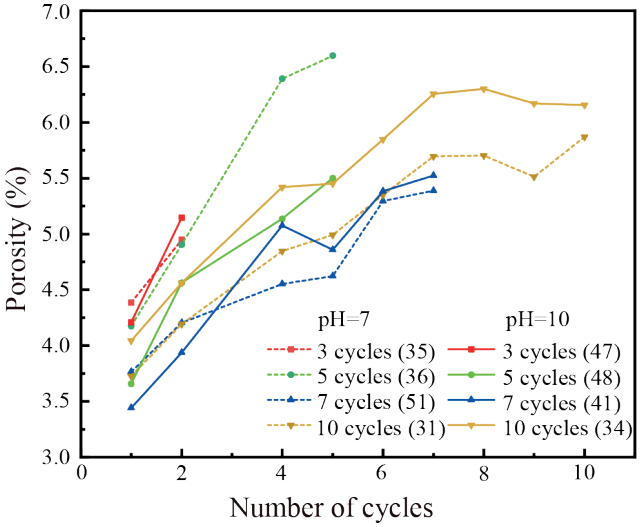

Fig. 5 porosity changes of rock specimens under different drying-wetting cycles

were dried in a 105 °C oven for 25 h and then cooled to an ambient temperature (25 °C). (5) Step 4 was repeated for 10 cycles. One specimen was removed from each of the two groups in the 1st, 3rd, 5th, 7th, and 10th cycles. The saturated specimens were used for the NMR tests, while the dried specimens were used for the SEM tests. Simultaneously, macroscopic morphology characteristics of the specimens were observed.

3 Results

3.1 Pore structure characteristics

The porosity (Fig. 5) and pore size distribution (Fig. 6 and Table 1) of sandstone can be accurately obtained through the NMR tests. On the basis of the pore radius classification method of measuring capillary pressure [23], the pores of sandstone were divided into small pores ($r < 0.15$ μm), medium pores (0.15 μm < r < 4 μm), and large pores ($r > 4$ μm).

For all the sandstone specimens, the original T_2 distribution curves presented three distinct peaks. Meanwhile, the proportion of small pores was the largest (62.4%–70.9%), followed by those of large pores (12.1%–22.5%) and medium pores (13.9%–17.9%) (Fig. 4). The porosity of sandstone generally exhibited an increasing trend with the number of wetting–drying cycles (N) increasing and tended to be stable when $N \geq 7$ (Fig. 5). In addition, the porosity increment of sandstone in the alkaline environment was generally higher than that in the neutral environment (except for Sample 36).

As the number of wetting–drying cycles increased, the medium pores of the specimens were the most affected by water–rock interaction, resulting in the weakening or disappearance of the second peak (Fig. 6). Compared with that in the original state, the number of pores (0.015–0.6 μm) increased significantly under the neutral wetting–drying cycle condition; and the more wetting–drying cycles, the larger the porosity increment (Fig. 7).

Although the effect of wetting–drying cycles on the pores (development of T_2 distributions) under two kinds of conditions was generally similar, there were still some differences. Under the alkaline condition, the pores (0.0005–0.015 μm) exhibited significant negative growth, and the increment of pores (0.3–10 μm) was considerably larger. In addition, the porosity increment (0.015–0.6 μm) under the alkaline condition was slightly lower than that under the neutral condition (Fig. 7).

3.2 Macroscopic morphology

During the wetting–drying cycle tests, rock debris spalling occurred on the surfaces of both groups of specimens, and spalling degree rose continuously with an increase in wetting–drying cycles. In addition, the spalling degree of the specimens in the neutral environment was significantly higher than that in the alkaline environment under the same number of wetting–drying cycles (N = 3, 5, 7, and 10) (Fig. 8).

3.3 Microscopic observation

Figs. 9 and 10 depict the SEM images of the specimens under two solution conditions. The particle size of the skeletal mineral quartz in the original sandstone specimen was larger (approximately 100–300 μm), with evident edges and corners (Figs. 9(a) and 10(a)). Except for a small number of quartz particles with extremely few straight micro-fissures

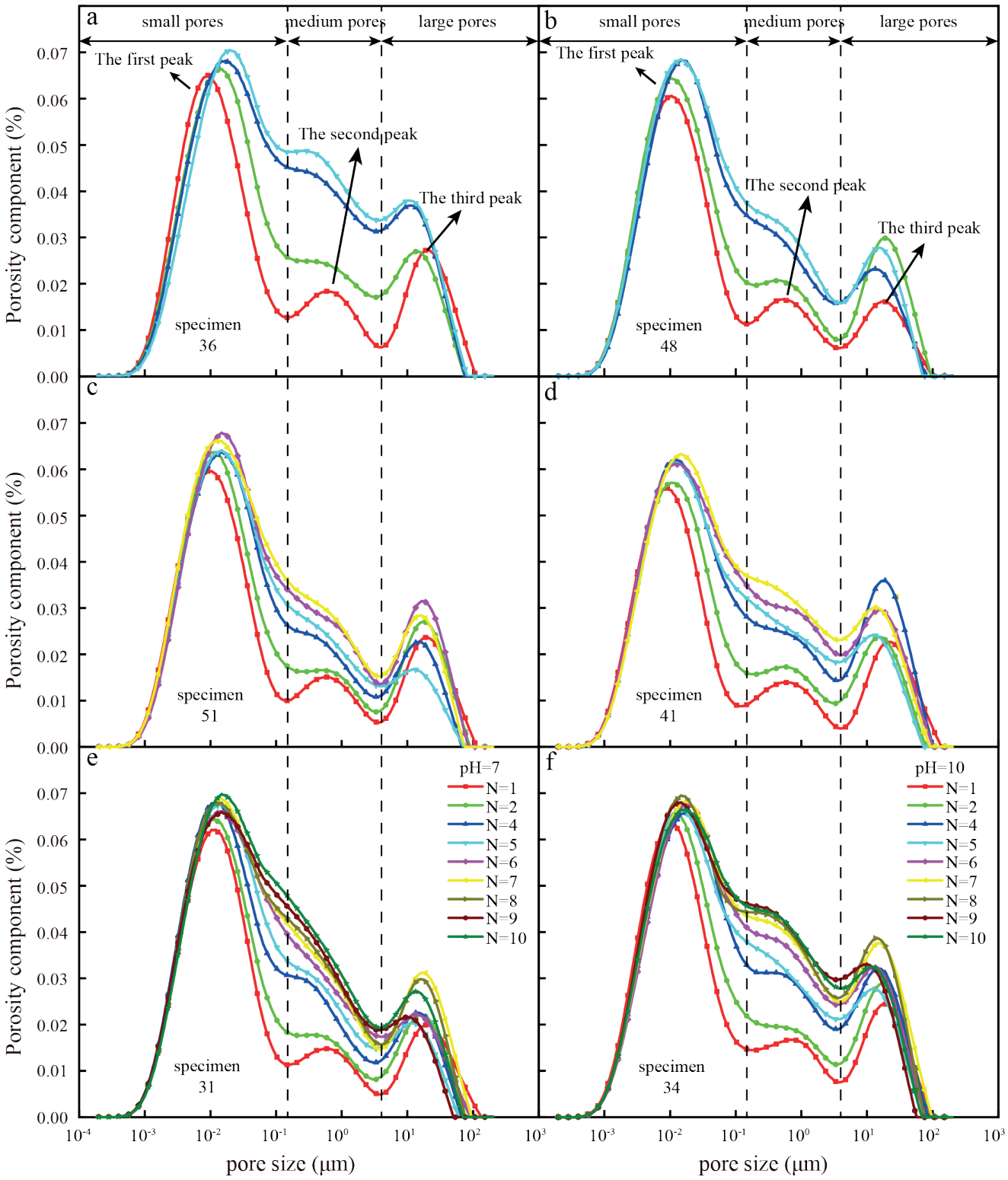

Fig. 6 T_2 spectrum distribution of rock specimens under different drying-wetting cycles (N)

(Fig. 9(b)), no micro-fissures occurred in most quartz particles (Fig. 10(b)), but many initial holes (approximately 0.1–0.5 μm) were observed (Figs. 9(b) and 10(b)). Meanwhile, clay minerals (kaolinite, montmorillonite, and illite) filled the gaps between the skeletal mineral quartz and attached to the surface of quartz particles (Figs. 9(a) and 10(a)).

Table 1 Pore types distribution of rock specimens under different drying-wetting cycles (N)

PH	specimen number	pore type	$N=1$ n_0/%	$N=3$ n_0/%	$N=4$ n_0/%	$N=5$ n_0/%	$N=6$ n_0/%	$N=7$ n_0/%	$N=8$ n_0/%	$N=9$ n_0/%	$N=10$ n_0/%
7	31	small pore	2.59	2.87	3.20	3.28	3.35	3.42	3.45	3.46	3.52
		medium pore	0.54	0.68	1.01	1.14	1.29	1.34	1.39	1.47	1.55
		large pore	0.60	0.64	0.64	0.57	0.71	0.94	0.86	0.59	0.80
		total porosity	3.73	4.19	4.85	4.99	5.35	5.70	5.70	5.51	5.87
10	34	small pore	2.70	2.92	3.18	3.25	3.29	3.37	3.41	3.42	3.39
		medium pore	0.65	0.82	1.27	1.38	1.58	1.70	1.74	1.82	1.80
		large pore	0.69	0.83	0.97	0.82	0.98	1.19	1.16	0.93	0.97
		total porosity	4.04	4.56	5.42	5.45	5.85	6.26	6.30	6.17	6.16
7	51	small pore	2.55	2.79	3.03	3.10	3.22	3.34			
		medium pore	0.54	0.65	0.90	1.03	1.17	1.23			
		large pore	0.69	0.76	0.63	0.50	0.91	0.82			
		total porosity	3.77	4.20	4.55	4.62	5.30	5.39			
10	41	small pore	2.28	2.58	2.96	2.98	3.12	3.13			
		medium pore	0.50	0.68	1.04	1.15	1.31	1.44			
		large pore	0.66	0.67	1.07	0.72	0.95	0.95			
		total porosity	3.44	3.94	5.08	4.86	5.38	5.52			
7	36	small pore	2.73	3.07	3.44	3.42					
		medium pore	0.66	1.04	1.83	2.00					
		large pore	0.78	0.80	1.12	1.18					
		total porosity	4.18	4.91	6.39	6.60					
10	48	small pore	2.60	2.94	3.24	3.39					
		medium pore	0.59	0.78	1.19	1.32					
		large pore	0.48	0.84	0.70	0.79					
		total porosity	3.66	4.56	5.14	5.50					

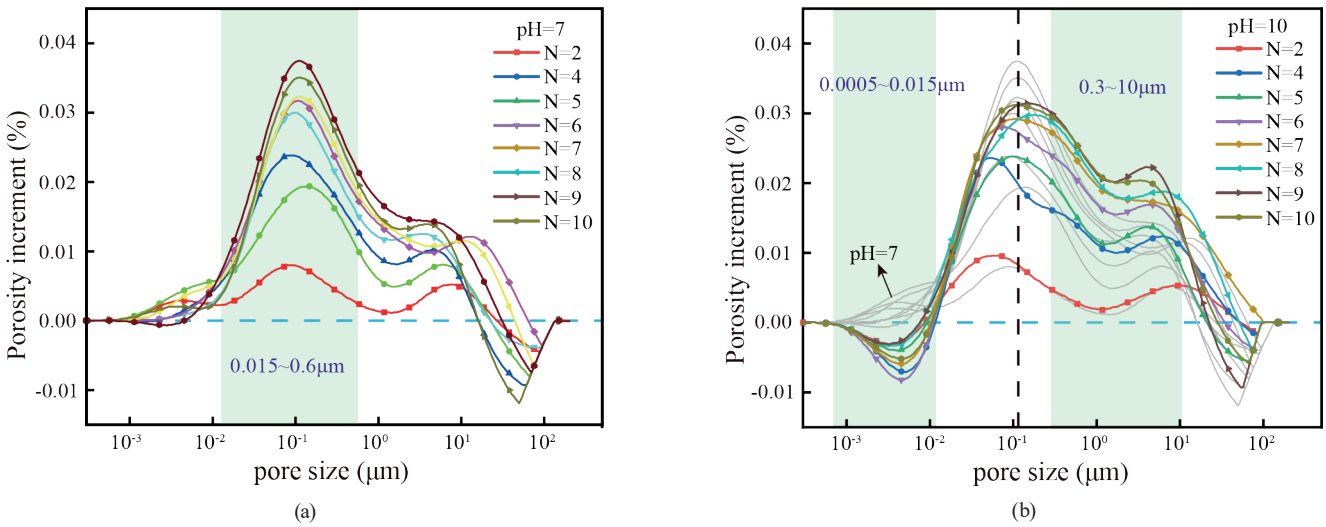

Fig. 7 Porosity increment at each size of rock specimens under different drying-wetting cycles (N); (a) pH = 7, (b) pH = 10

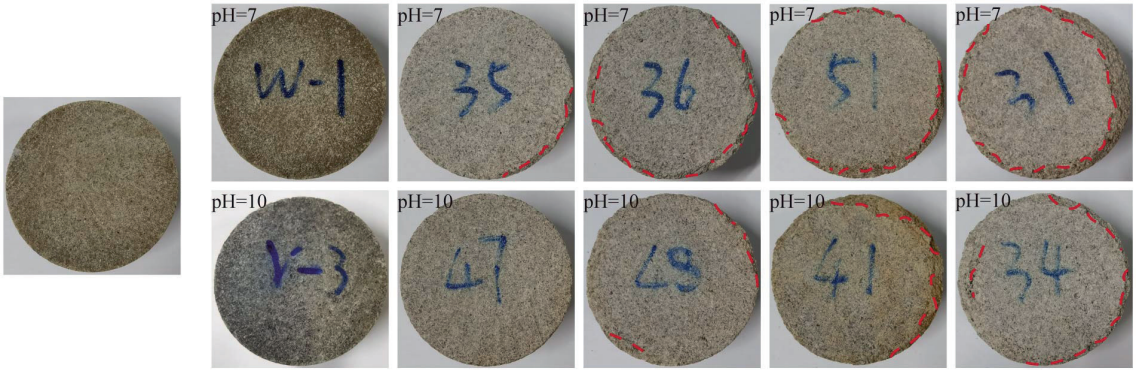

(a) $N = 0$ (b) $N = 1$ (c) $N = 3$ (d) $N = 5$ (e) $N = 7$ (f) $N = 10$

Fig. 8 Change of surface morphology of sandstone specimens under different drying-wetting cycles (N)

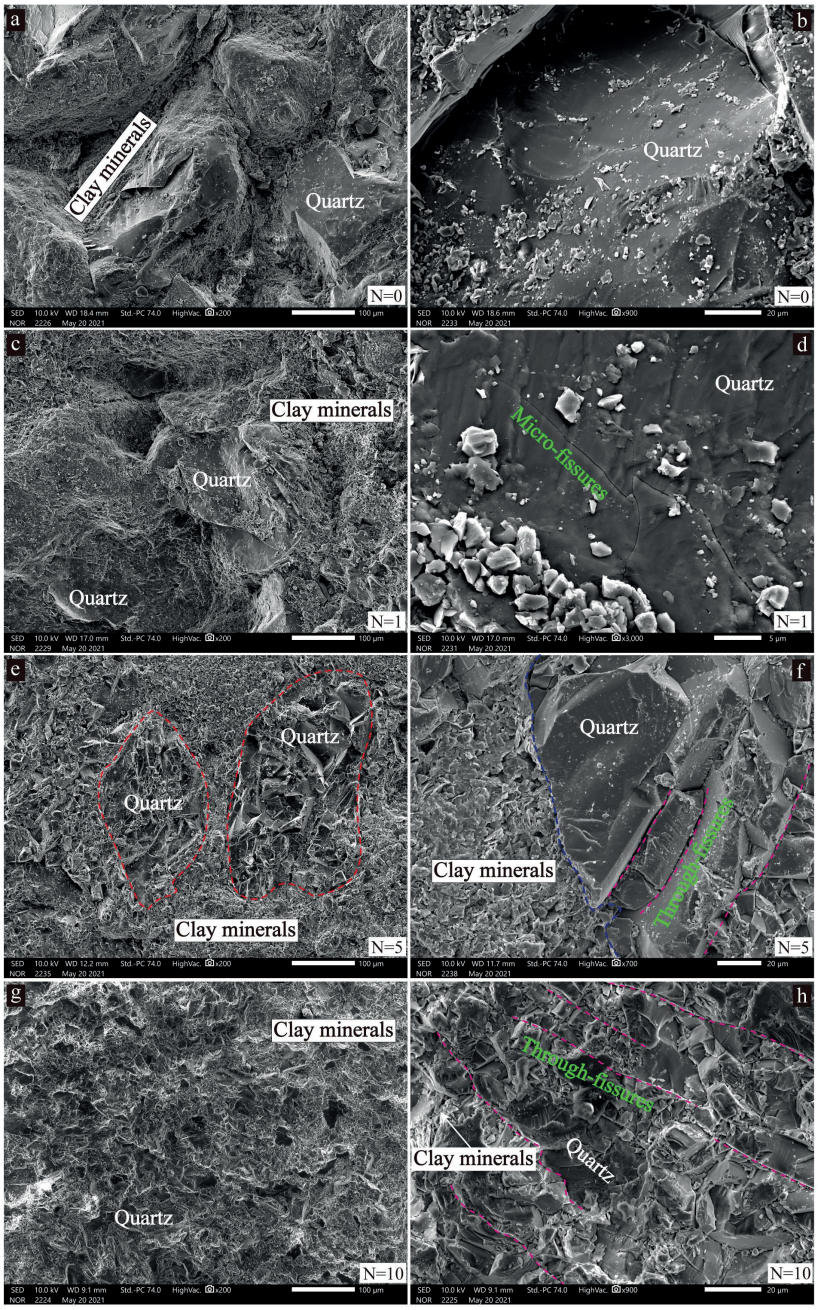

Fig. 9 SEM images of sandstone specimens under different drying-wetting cycles (N) at pH = 7

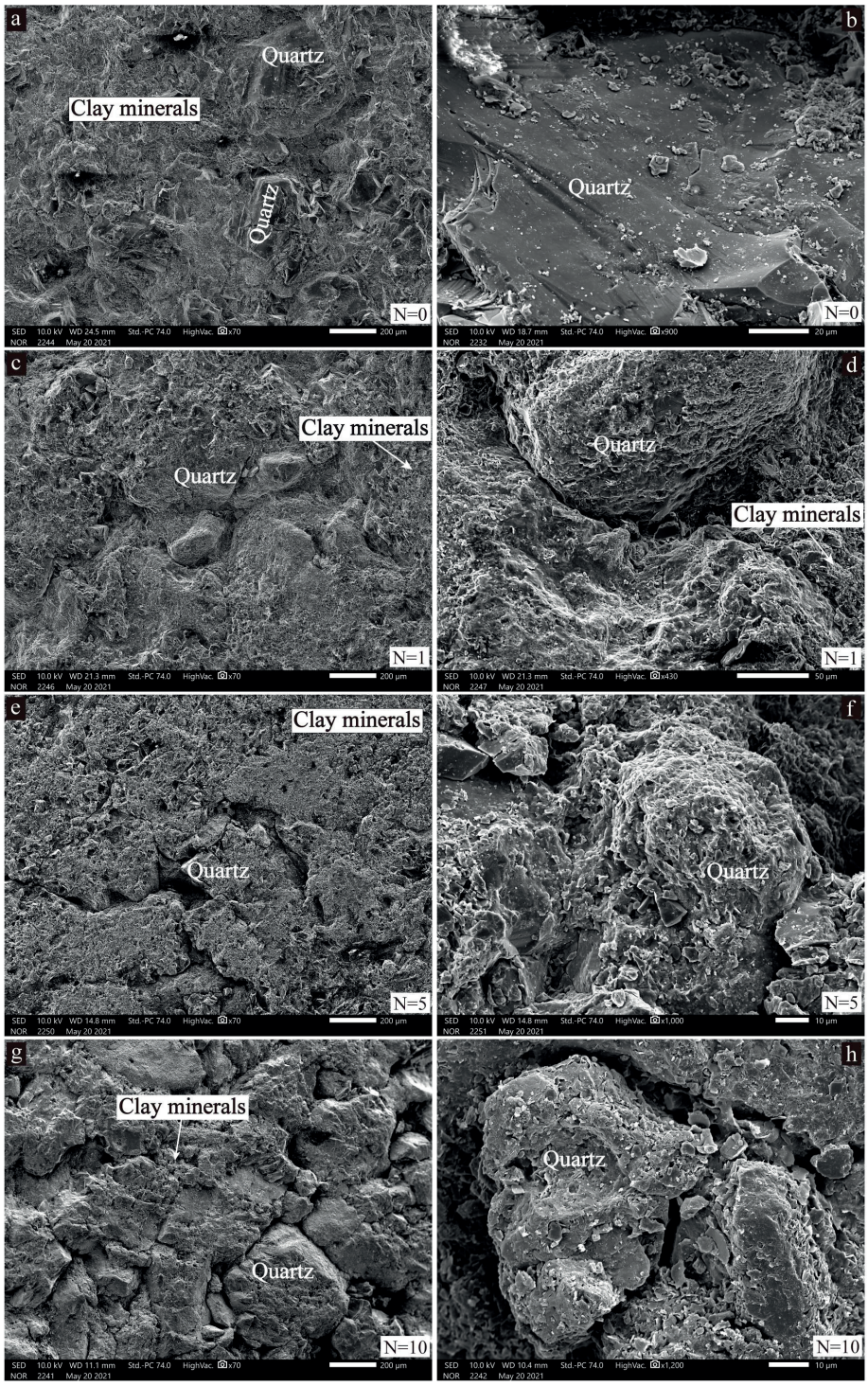

Fig. 10 SEM images of sandstone specimens under different drying-wetting cycles (N) at pH = 10

Under the neutral wetting–drying cycle condition (pH = 7), the microstructures of the specimens changed significantly. The quartz particles became increasingly broken (Fig. 9) with an increase in the number of wetting–drying cycles (N). When N = 1, no significant change occurred in the morphology of quartz particles (Fig. 9(c)), but many sprouting and crossing micro-fissures (approximately 0.1–0.2 μm) connected inside the quartz particles (Fig. 9(d)). When N = 5, quartz particles were considerably damaged, but their initial surface profiles could still be distinguished (Fig. 9(e)). Simultaneously, micro-fissures developed within quartz particles and connected with one another to form larger micro-fissures (approximately 5–30 μm), leading to the breakage

of quartz particles (Fig. 9(f)). Notably, clear boundaries existed between quartz particles and clay minerals, indicating that quartz did not undergo strong chemical reactions. When N = 10, quartz particles tended to be broken completely (approximately 5–30 μm) (Fig. 9(g)), and the internal through-fissures of different quartz particles were interconnected to form macro through-cracks (Fig. 9(h)).

Compared with the specimens in the neutral water environment, the alkaline water–rock interaction exhibited a significant difference in the mesoscopic modification of sandstone. In an alkaline water environment, the wetting–drying cycles not only resulted in the dissolution of quartz particles but also led to the coalescence and extension of micro-fissures between framework minerals. As shown in Figs. 10(c)–10(e), the micro-fissures between framework minerals gradually connected into larger micro-cracks as the number of wetting–drying cycles increased. In contrast with the crushing of quartz particles caused by a neutral wetting–drying cycle condition, no evident extrusion crushing of quartz particles occurred in the alkaline water environment. However, the dissolution of quartz particles was apparent, and a large number of clay minerals filled or attached to the dissolution pits formed on the surface of quartz particles (Figs. 10(d), 10(f), and (h)).

4 Discussion

The rock pore structure is one of the important factors that affect rock strength [15]. Thus, it is a key to determining the deterioration mechanism of rocks that the rock pore structure and its evolution process under wetting–drying cycles. Under the water–rock interaction, the chemical erosion [24–26] and physical expansion [6, 26–27] of minerals are the primary controlling factors that affect the evolution of pore structures. Chemical erosion mostly changes the species or mesoscopic morphology of minerals through dissolution and hydrolysis. In contrast, physical expansion alters the mesostructure of rocks through water swelling and the expansion of clay minerals. Although the two methods can lead to the modification of rock pore structures, essential differences occur in the method and process of mineral transformation. Therefore, the key to studying laws for the rock pore structures development is to determine the evolution process of mineral meso-morphology.

4.1 Pore characteristics of sandstone with wetting–drying cycles

Compared with other types of sandstone in TGRA [28–29], the sandstone specimens only consist of quartz (69.8%) and clay minerals (30.2%), which lack minerals that easily react with water, such as feldspar and mica. In a neutral water environment (pH = 7), quartz and clay minerals basically do not react with water [26], indicating that chemical erosion exerts limited influence on the evolution of sandstone pore structure. On the other hand, clay minerals have properties of water absorption and expansion [9]. However, the morphology of framework minerals is rarely described. Due to the expansion of clay minerals under the water condition, combined with the clay minerals distributed among framework minerals (quartz) like a reticulum (Fig. 2) in this study, the pores have firstly been filled, and then the framework minerals have been continuously squeezed. This results in the initiation of secondary cracks (Fig. 9(d)) and the gradual increase in the number of smaller pores (0.0005–0.015 μm) (Fig. 7). Therefore, under neutral water–rock interaction, the physical expansion is the fundamental factor that leads to the deterioration of the sandstone.

In addition, as the number of wetting–drying cycles increases, quartz particles experience the initiation and expansion of micro-cracks until macro-cracks coalesce, exhibiting a progressive failure mode of quartz particles from the interior to the exterior (Fig. 11(a)). This process gradually increases the number of pores of all sizes, particularly small and medium ones (0.01–1 μm). Meanwhile, the rock debris spalling phenomenon on the sample surface becomes increasingly evident with an increase in wetting–drying cycles (Fig. 8). This also suggests the deterioration of the internal structure of the specimens because of the "saturation–dehydration" process of clay minerals. On one hand, a high-stress environment will be formed under the saturation condition. This results in more new micro-cracks developed within individual quartz grains (Fig. 9). On the other hand, a low-stress state owing to the drying shrinking of clay minerals leads to the tensile fracture damage of sandstone [27]. Thus, under wetting–drying cycles, the clay minerals have been experienced the cyclic states of "dilatation–contraction" and "high–low stress", leading to crack propagation and coalescence in the interior of the rock. Finally, connection capability between minerals in the rock is reduced, resulting in the deterioration of sandstone pore structure and rock debris spalling.

4.2 Role and effect of chemical erosion in sandstone deterioration

Due to the high contents of clay minerals (30.2%) in the specimens, the process of "expansion–contraction" caused

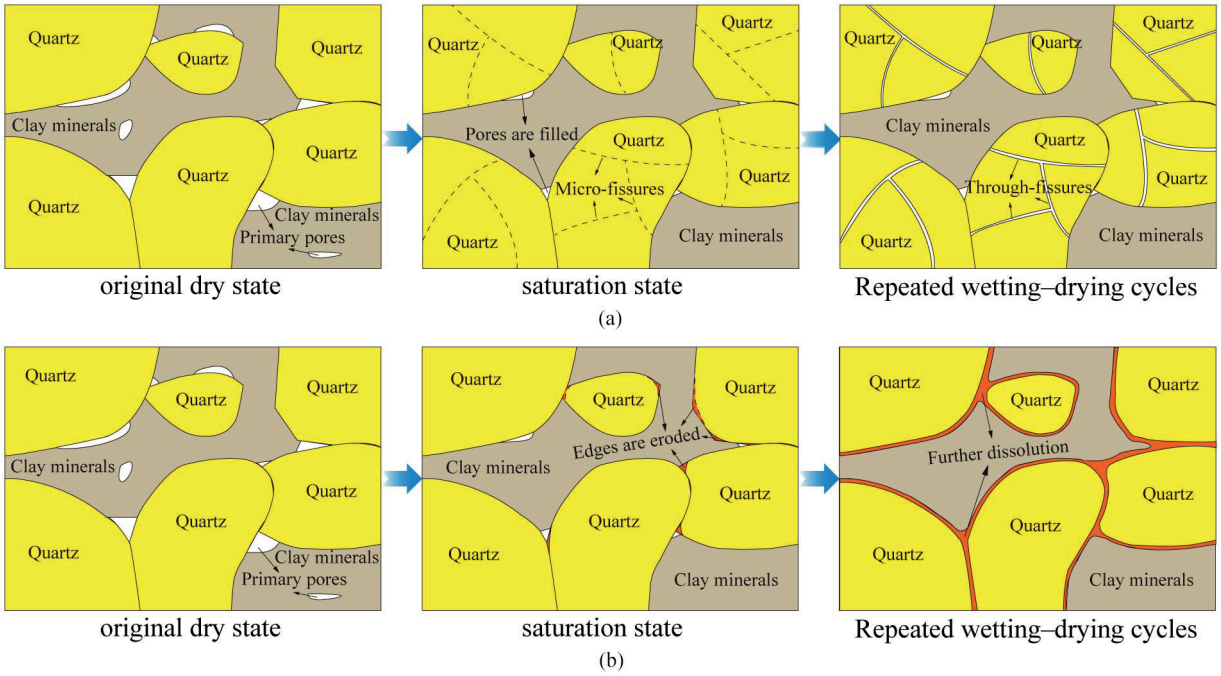

Fig. 11 Model diagram of the mineral evolution process of sandstone; (a) neutral wetting-drying cycles, (b) alkaline wetting-drying cycles

by the "saturation–dehydration" of clay minerals is the major factor that causes sandstone deterioration whether in a neutral or alkaline water environment. The similar T_2 spectrum characteristics of specimens under neutral and alkaline water conditions also support this view (Fig. 6). However, compared to the T_2 spectrum distributions of the specimens in a neutral water environment, the smaller pores and fractures (0.0005–0.015 μm) in the specimens show distinctly negative growth under alkaline conditions (Fig. 7). This reflects the differences in the damage way of the sandstone in neutral and alkaline water environments. The micro-surface texture of quartz interacted with hydroxide ion of alkaline water shows remarkable corroded pores (Fig. 10), instead of the micro-cracks in the quartz (Fig. 9) caused by physical mechanics in neutral water (discussion in Section 4.1). Such phenomena reveals that the dissolution leads to the different damage way of micro-structure for the specimens reacted with alkaline water. When quartz is attacked by the hydroxide ion of alkaline water, it dissolves as follow [25]:

$$SiO_2 + 2OH^- \rightarrow H_2SiO_4^{2-} (\Delta G = -15.785\,\text{kJ/ mol}) . \quad (1)$$

The dissolution of the quartz makes many ions free from the framework and go into pore-water, leading the increase in the porosity of the specimens. Due to such erosion process altered minerals from the exterior to the interior (Fig. 11(b)), it not only promotes the expansion of smaller pores and fractures to form larger ones, resulting in the negative growth of smaller pores and fractures (Fig. 7), but also leads to the more increment of larger pores and fractures (0.3–10 μm) in the alkaline water environment than that in the neutral water environment (Fig. 7). In addition, the pores and fractures formed by chemical erosion provide more available space for clay minerals during the water absorption and expansion process. Such "buffering effect" prevents quartz particles from being crushed in microcosm (Fig. 10) and makes rock debris spalling evidently weaker than that in the neutral water environment in macroscopic (Fig. 8).

Although the chemical erosion can relieve the compressive stress from the clay minerals expansion in the water, the "water absorption expansion–water loss contraction" of clay minerals further leads to pore expansion, which increases the reaction area and promotes further chemical erosion. Therefore, wetting–drying cycles can effectively promote the development of pores in sandstone and then significantly weaken the cementing property between framework minerals, eventually causing rocks to evolve gradually into a loose porous structure.

4.3 Relationship between the swelling amount and swelling force of clay minerals

Expansive rocks (soils) exert macroscopically expansive effects due to the water absorption of clay minerals. Under unconstrained conditions, this expansion effect is completely converted into volume expansion (such as the free

swelling rate test); however, if rigid structures or load constraints exist, then the expansion effect is partially converted into expansion, and the rest is converted into a general swelling force (such as the swelling force test) [30]. For the argillaceous quartz sandstone used in this study, the framework mineral quartz not only supports rock structures, but also restricts the clay minerals from fully expanding. Therefore, in accordance with the tests of a pressurized expansion method [30], we establish the relationship between the swelling amount and swelling force to explore the meso-mechanical relationship between swelling force and porosity.

When constraints exist, the test data of the remolded expansive rock (soils) [31] indicate that the logarithmic swelling force (P_e) is negatively linearly correlated with the expansive strain (ε):

$$\lg P_e = A\varepsilon + B\left(|R| > 0.99\right), \tag{2}$$

where A and B are regression coefficients ($A < 0$ and $B > 0$).

Consider the following conditions:

1) When strain (ε) is 0 (maximum constraint), the maximum swelling force, $\lg P_{e\max} = B$, is obtained.

2) When strain (ε) is the maximum (completely unconstrained), it is also the unloaded expansion rate (δ_H), and thus, the swelling force is $P_e(\delta_H)$. Equation (2) can be expressed as $\lg P_e(\delta_H) = A\delta_H + B$. A positive linear correlation exists between unloaded expansion rate (δ_H) and water content (w), as follows [31]:

$$\delta_H = aw + b\left(|R| > 0.95\right). \tag{3}$$

Moreover, the relation among expansion strain (ε), swelling force (P_e), and unloaded expansion rate (δ_H) is established as follows:

$$\varepsilon = f\left(P_e\right)\delta_H, \tag{4}$$

where $f(P_e)$ is the function of swelling force (P_e).

3) When strain (ε) is ε (partial constraint): $\lg P_e = A\varepsilon + B$.

According to the three aforementioned conditions, the relation between swelling force (P_e) and expansion strain (ε) can be obtained as follows:

$$f\left(P_e\right) = \frac{\lg P_e - \lg P_{e\max}}{\lg P_e\left(\delta_H\right) - \lg P_{e\max}}. \tag{5}$$

Given that swelling force is close to zero under no load, δ_H is set as the swelling rate under 1 kPa restraint stress, expressed as $P_e(\delta_H)$ =1 kPa, to simplify the calculation. Then substitute this condition into Eq. (5):

$$f\left(P_e\right) = 1 - \frac{\lg P_e}{\lg P_{e\max}}. \tag{6}$$

In addition, in accordance with Eq. (3), the influence of water content change (Δw) during the absorption and expansion process can be considered as:

$$\Delta\delta_H = a\Delta w. \tag{7}$$

Then, Eq. (6) and (7) are substituted into Eq. (4) as follows:

$$\lg P_e = -\frac{\lg P_{e\max}}{a\Delta w}\varepsilon + \lg P_{e\max}, \tag{8}$$

Where $-(\lg P_{e\max} / a\Delta w)$ and $\lg P_{e\max}$ are the regression coefficients A and B in Eq. (2), respectively.

$P_{e\max}$ is determined by the material properties and initial state of clay minerals, representing the maximum stress value without deformation. Thus, coefficient B can be regarded as a constant. Furthermore, Eq. (3) shows that coefficient A is jointly controlled by coefficient B and $\Delta\delta_H$. Therefore, in combination with Eq. (7), it can be inferred that coefficient A is determined by water content change (Δw).

Combined with this experimental study, Δw can be regarded as a constant (saturated soaking), and thus, $-(\lg P_{e\max} / a\Delta w)$ is also a constant. Consequently, a conclusion can be drawn from Eq. (8) that swelling force is only affected by expansion strain and negatively correlated with expansion strain. Moreover, expansion strain (ε) is the maximum space available after the water absorption and expansion of clay minerals. Meanwhile, when the deformation of framework minerals (quartz) is extremely small, the maximum expansion strain of clay minerals can reflect the development degree of rock pores, and swelling force is also closely related to rock porosity.

In a neutral environment, the reaction rate between minerals and solution is extremely slow, and thus, the influence of water–rock chemistry on rock porosity can be nearly disregarded. Accordingly, the expandable strain (ε) of clay minerals after water absorption is limited, leading to a larger swelling force inside the sandstone and resulting in the extrusion and breakage of quartz particles. By contrast, the dissolution of quartz significantly increases the porosity of sandstone in an alkaline environment, and the expandable strain (ε) of clay minerals also increases after water absorption. Therefore, the swelling force inside the rock is considerably reduced in this case, which is also the primary reason why quartz particles are not evidently crushed.

5 Conclusions

1. The wetting–drying cycles in both neutral and alkaline environments can increase the porosity of sandstone, and the increase in amplitude is higher in an alkaline water environment. In particular, water–rock interaction in a neutral environment primarily causes a huge increase in medium porosity (0.015–0.6 μm). In an alkaline environment, water–rock interaction results in significant growth of large pores (0.3–10 μm) and slightly negative growth of small pores (0.0005–0.015 μm), exhibiting differences in pore structures.
2. Under the condition of wetting–drying cycles in a neutral environment, the "saturation–dehydration" of clay minerals causes the interior of sandstone to experience a "dilatation–contraction" process. This process demonstrates that new micro-cracks are not only initiated under the action of swelling force, but micro-cracks also gradually connect to form through-cracks, leading to the breakage of framework mineral quartz particles.
3. In an alkaline water environment, quartz particles are significantly dissolved, resulting in a significant increase in sandstone porosity. Although this effect provides a buffer space for the absorption and expansion of clay minerals, which weakens swelling force inside the sandstone, it also continuously weakens cementation capability between framework minerals and causes the rock to evolve into a loose porous structure.
4. Compared with previous research focusing on the relationship between the mechanical properties and microstructural changes, our study has suggested that the alteration behavior of minerals is an important factor in controlling the evolution of the mesoscopic structure of rocks. Therefore, the study of water–rock interaction in a reservoir's fluctuation zone and the prevention and control of possible geological disasters should be based on mineralogy analysis combined with water environment and other factors.

Acknowledgement

This work was supported by the National Natural Science Foundation of China (41903023), the Research Foundation of high-level talents of Three Gorges University, the Open Research Fund for the National Field Observation and Research Station of Landslides in Three Gorges Reservoir Area of Yangtze River (Grant No. 2018KTL07), the Special Fund of National Field Observation and Research Station of Landslides in Three Gorges Reservoir Area of Yangtze River (Grant No. 2020179), the Research on Geological Hazard Survey in the Slope Deterioration Zone in Three Gorges Reservoir Area of Yangtze River in Yichang, Hubei Province (Grant No. SDH2021102), and 111 Project of Hubei Province (Grant Number 2021EJD026). Thoughtful reviews and the comments of editors and anonymous reviewers helped us to strengthen the manuscript.

References

[1] Tang, H. M., Wasowski, J., Juang, C. H. "Geohazards in the three Gorges Reservoir Area, China – Lessons learned from decades of research", Engineering Geology, 261, 105267, 2019. https://doi.org/10.1016/j.enggeo.2019.105267

[2] Wang, J. G., Xiang, W., Lu, N. "Landsliding triggered by reservoir operation: a general conceptual model with a case study at Three Gorges Reservoir", Acta Geotechchnica, 9, pp. 771–788, 2014. https://doi.org/10.1007/s11440-014-0315-2

[3] Luo, Z., Li, J., Jiang, Q., Zhang, Y., Huang, Y., Assefa, E., Deng, H. "Effect of the Water-Rock Interaction on the Creep Mechanical Properties of the Sandstone Rock", Periodica Polytechnica Civil Engineering, 62(2), pp. 451–461, 2018. https://doi.org/10.3311/PPci.11788

[4] Sun, Q., Zhang, Y. "Combined effects of salt, cyclic wetting and drying cycles on the physical and mechanical properties of sandstone", Engineering Geology, 248, pp. 70–79, 2019. https://doi.org/10.1016/j.enggeo.2018.11.009

[5] Song, Z., Sun, L., Cheng, S., Liu, Z., Tan, J., Ning, F. "Experimental Study on the Property Degradation and Failure Mechanism of Weakly Cemented Sandstone under Dry-Wet Cycles", Advances in Materials Science and Engineering, 2022, Article ID 9431319, 2022. https://doi.org/10.1155/2022/9431319

[6] Zhang, H., Lu, K., Zhang, W., Li, D., Yang, G. "Quantification and acoustic emission characteristics of sandstone damage evolution under dry–wet cycles", Journal of Building Engineering, 48, 103996, 2022. https://doi.org/10.1016/j.jobe.2022.103996

[7] Liu, X., Jin, M., Li, D., Zhang, L. "Strength deterioration of a Shaly sandstone under dry–wet cycles: a case study from the Three Gorges Reservoir in China", Bulletin of Engineering Geology and the Environment, 77, pp. 1607–1621, 2018. https://doi.org/10.1007/s10064-017-1107-3

[8] Zhang, B. Y., Zhang, J. H., Sun, G. L. "Deformation and shear strength of rockfill materials composed of soft siltstones subjected to stress, cyclical drying/wetting and temperature variations", Engineering Geology, 190, pp. 87–97, 2015. https://doi.org/10.1016/j.enggeo.2015.03.006

[9] Wang, L. L., Bornert, M., Héripré, E., Yang, D. S., Chanchole, S. "Irreversible deformation and damage in argillaceous rocks induced by wetting/drying", Journal of Applied Geophysics, 107, pp. 108–118, 2014.
https://doi.org/10.1016/j.jappgeo.2014.05.015

[10] Xie, K., Jiang, D., Sun, Z., Chen, J., Zhang, W., Jiang, X. "NMR, MRI and AE Statistical Study of Damage due to a Low Number of Wetting–Drying Cycles in Sandstone from the Three Gorges Reservoir Area", Rock Mechanics and Rock Engineering, 51, pp. 3625–3634, 2018.
https://doi.org/10.1007/s00603-018-1562-6

[11] Wang, C., Pei, W., Zhang, M., Lai, Y., Dai, J. "Multi-scale Experimental Investigations on the Deterioration Mechanism of Sandstone Under Wetting–Drying Cycles", Rock Mechanics and Rock Engineering, 54, pp. 429–441, 2021.
https://doi.org/10.1007/s00603-020-02257-2

[12] Li, H., Zhong, Z., Liu, X., Sheng, Y., Yang, D. "Micro-damage evolution and macro-mechanical property degradation of limestone due to chemical effects", International Journal of Rock Mechanics and Mining Sciences, 110, pp. 257–265, 2018
https://doi.org/10.1016/j.ijrmms.2018.07.011

[13] Guo, Y. "Research on the damage mechanism of siltstone from Xiangxi Riverbank in drying and wetting cycle", MSc Thesis, China University of Geosciences, 2013. (in Chinese) [online] Available at: http://d.et.wanfangdata.com.cn/Thesis/Y2436899

[14] Liu, X. R., Yuan, W., Fu, Y., Wang, Z. J., Miao, L. L. "Porosity evolution of sandstone dissolution under wetting and drying cycles", Chinese Journal of Geotechnical Engineering, 40(3), pp. 527–532, 2018. (in Chinese)
https://doi.org/10.11779/CJGE201803017

[15] Chen, X., He, P., Qin, Z. "Damage to the microstructure and strength of altered granite under wet–dry cycles", Symmetry, 10(12), 716, 2018.
https://doi.org/10.3390/sym10120716

[16] Qin, Z., Fu, H., Chen, X. "A study on altered granite meso-damage mechanisms due to water invasion-water loss cycles", Environmental Earth Sciences, 78, 428, 2019
https://doi.org/10.1007/s12665-019-8426-6

[17] Fairhurst, C. E., Hudson, J. A. "Draft ISRM suggested method for the complete stress-strain curve for intact rock in uniaxial compression", International Journal of Rock Mechanics & Mining Science, 36(3), pp. 281–289, 1999.
https://doi.org/10.1016/S0148-9062(99)00006-6

[18] Tan, M. J., Zhao, W. J. "Description of carbonate reservoirs with NMR log analysis method", Progress in Geophysics, 21(02), pp. 489–493, 2006. (in Chinese)
https://doi.org/10.3969/j.issn.1004-2903.2006.02.023

[19] Yu, J., Zhang, X., Cai, Y. Y., Liu, S. Y., Tu, B. X. "Meso-damage and mechanical properties degradation of sandstone under combined effect of water chemical corrosion and freeze-thaw cycles", Rock and Soil Mechanics, 40(02), pp. 455–464, 2019. (in Chinese)
https://doi.org/10.16285/j.rsm.2017.1450

[20] Cerco, C. F., Threadgill, T., Noel, M. R., Hinz, S. "Modeling the pH in the tidal fresh Potomac River under conditions of varying hydrology and loads", Ecological Modelling, 257, pp. 101–112, 2013.
https://doi.org/10.1016/j.ecolmodel.2013.02.011

[21] Yang, Z., Liu, D., Ji, D., Xiao, S. "Influence of the impounding process of the Three Gorges Reservoir up to water level 172.5 m on water eutrophication in the Xiangxi Bay", Science China Technological Sciences, 53, pp. 1114–1125, 2010.
https://doi.org/10.1007/s11431-009-0387-7

[22] Wang, Q., Zhou, L., Little, S. H., Liu, J., Feng, L., Tong, S. "The geochemical behavior of Cu and its isotopes in the Yangtze River", Science of the Total Environment, 728, 138428, 2020.
https://doi.org/10.1016/j.scitotenv.2020.138428

[23] Li, J. L., Zhu, L. Y., Zhou, K. P., Liu, H. W., Cao, S. P. "Damage characteristics of sandstone pore structure under freeze-thaw cycles", Rock and Soil Mechanics, 40(9), pp. 3524–3532, 2019. (in Chinese)
https://doi.org/10.16285/j.rsm.2018.1066

[24] Su, X., Tang, H., Huang, L., Shen, P., Xia, D. "The role of pH in red-stratum mudstone disintegration in the Three Gorges reservoir area, China, and the associated micromechanisms", Engineering Geology, 279, 105873, 2020
https://doi.org/10.1016/j.enggeo.2020.105873

[25] Yuan, W., Liu, X., Fu, Y. "Chemical thermodynamics and chemical kinetics analysis of sandstone dissolution under the action of dry–wet cycles in acid and alkaline environments", Bulletin of Engineering Geology and the Environment, 78, pp. 793–801, 2019.
https://doi.org/10.1007/s10064-017-1162-9

[26] Qiao, L. P., Liu, J., Feng, X. T. "Study on damage mechanism of sandstone under hydro-physico-chemical effects", Chinese Journal of Rock Mechanics and Engineering, 26(10), pp. 2117–2124, 2007. (in Chinese)
https://doi.org/10.3321/j.issn:1000-6915.2007.10.023

[27] Wang, Z., Shen, M. R., Liu, A. "Water-rock interaction characteristics and softening mechanism of calcareous mudstone", Journal of Southwest Jiaotong University, 50(06), pp. 1061–1066, 2015. (in Chinese)
https://doi.org/10.3969/j.issn.0258-2724.2015.06.012

[28] Zhou, M., Li, J., Luo, Z., Sun, J., Xu, F., Jiang, Q., Deng, H. "Impact of water–rock interaction on the pore structures of red-bed soft rock", Scientific Reports, 11, 7398, 2021.
https://doi.org/10.1038/s41598-021-86815-w

[29] Zhang, Z., Jiang, Q., Zhou, C., Liu, X. "Strength and failure characteristics of Jurassic Red-Bed sandstone under cyclic wetting-drying conditions", Geophysical Journal International, 198(2), pp. 1034–1044, 2014.
https://doi.org/10.1093/gji/ggu181

[30] Ding, Z. Z., Zheng, Y. R., Li, L. S. "Trial study on variation regularity of swelling force", Rock and Soil Mechanics, 28(7), pp.1328–1332, 2007. (in Chinese)
https://doi.org/10.16285/j.rsm.2007.07.008

[31] Liu, J. D., Li, Q. Y., Gong, B. W. "Swelling properties of expansive rock in Middle Route Project of South-to-North Water Diversion", Chinese Journal of Geotechnical Engineering, 33(5), pp. 826–830, 2011. (in Chinese) [online] Available at: http://www.cnki.com.cn/Article/CJFDTotal-YTGC201105030.htm